



Research Article

**Investigation of Radiation Effects on Cr-Co-Ni Alloys Used in Dental Applications by Monte Carlo Simulation**

Doğan DURNA<sup>1</sup>, Bünyamin AYGÜN\*<sup>2</sup>, Abdulhalik KARABULUT<sup>3</sup>

<sup>1</sup>Ataturk University, Dentistry Faculty, Dentomaxillofacial Radiology, Department, 25700, Erzurum, Türkiye

<sup>2</sup>Ağrı İbrahim Çeçen University, Vocational School, Electronics and Automation Department, Postal Code, Ağrı, Türkiye

<sup>3</sup>Ataturk and Ağrı İbrahim Çeçen University, Science Faculty Physics, Department, 25700, Erzurum, Türkiye  
Doğan DURNA, ORCID No: 0000-0001-5341-6024, Bünyamin AYGÜN, ORCID No: 0000-0002-9384-1540,  
Abdulhalik KARABULUT, ORCID No: 0000-0003-2290-9007

\*Corresponding author e-mail: baygun@agri.edu.tr

**Article Info**

Received: 22.07.2024

Accepted: 20.08.2024

Online August 2024

DOI: [10.53433/yyufbed.1520230](https://doi.org/10.53433/yyufbed.1520230)

**Keywords**

Denture,  
Implant,  
Monte Carlo,  
Neutron radiation

**Abstract:** Radiation is used in dental applications, both in any tumor treatment and oral diagnosis. Especially boron -neutron treatment mostly uses brain and larynx cancer treatment. In recent years, denture restoration has become important in combating tooth decay and tooth loss. Many alloys are used for both restoration and medical purposes, with cobalt-chromium (Co-Cr) alloys seeing increasing use. These alloys are favored because they offer good resistance to corrosion and mechanical wear. Toxicity and radiation resistance are crucial properties of these alloys in oral applications. Individuals with chrome-coated implants and restorations may be exposed to radiation during diagnostic procedures while working in nuclear facilities or undergoing radiotherapy treatments like boron neutron therapy. The epithermal and fast neutron interaction parameters, including effective removal cross-section, half-value layer, mean free path, and transmission number, have been determined for dentures used in medical applications with three types of Co-Cr alloys. These parameters and the emitted secondary radiation were calculated using the effective semi-experimental Monte Carlo simulation software, GEANT4. It was determined that the first type of alloys are best suited for oral restorations in people exposed to radiation.

**Dental Uygulamalarda Kullanılan Cr-Co-Ni Alaşımlarında Radyasyonun Etkilerinin Monte Carlo Simülasyonu ile Araştırılması**

**Makale Bilgileri**

Geliş: 22.07.2024

Kabul: 20.08.2024

Online Ağustos 2024

DOI: [10.53433/yyufbed.1520230](https://doi.org/10.53433/yyufbed.1520230)

**Anahtar Kelimeler**

İmplant,  
Monte Carlo,  
Nötron radyasyonu,  
Protez

**Öz:** Radyasyon diş hekimliği uygulamalarında hem her türlü tümör tedavisinde hem de ağız yoluyla teşhiste kullanılmaktadır. Özellikle bor-nötron tedavisinde çoğunlukla beyin ve gırtlak kanseri tedavisinde kullanılmaktadır. Son yıllarda diş çürüğü ve diş kaybıyla mücadelede protez restorasyonu önem kazanmıştır. Birçok alaşım hem restorasyon hem de tıbbi amaçlar için kullanılmakta özellikle kobalt-krom (Co-Cr) alaşımlarının kullanımı giderek artıyor. Bu alaşımlar, korozyona ve mekanik aşınmaya karşı iyi bir direnç sundukları için tercih ediliyor. Toksikite ve radyasyon direnci bunların çok önemli özellikleridir. Oral uygulamalarda alaşımlar krom kaplı implantlara ve restorasyonlara sahip kişiler, nükleer tesislerde çalışırken veya bor nötron tedavisi gibi radyoterapi tedavilerine tabi tutulurken teşhis prosedürleri sırasında radyasyona maruz kalabilirler. Üç tip Co-Cr alaşımı ile tıbbi uygulamalarda kullanılan protezler için epitermal ve hızlı nötron etkileşimi parametreleri etkili uzaklaştırma kesiti, yarı değer katmanı, ortalama serbest yol ve iletim sayısı belirlendi. Bu parametreler ve yayılan ikincil radyasyon, etkili yarı deneysel Monte Carlo simülasyonu kullanılarak hesaplandı. GEANT4 yazılımı ile radyasyona maruz kalan kişilerde ağız restorasyonları için birinci tip alaşımların en uygun olduğu belirlendi.

## 1. Introduction

Neutrons are used in various applications such as nuclear medicine diagnosis and treatment, nuclear power plants, materials science, and space research (Nazarov et al., 2020). Staff working in these areas can be exposed to neutron leaks. If they have any denture implants or restorative chrome coatings, neutrons can interact with these materials, producing secondary radiation that may cause health problems. Cobalt-chromium (Co-Cr) alloys have been used in implant and restorative treatment applications in dentistry for a long time. These alloys contain Cr and Co, along with other metals such as nickel (Ni), manganese (Mn), silicon (Si), molybdenum (Mo), iron (Fe), and tungsten (W) (Kassapidou et al., 2017). These Co-Cr alloys consist of 2–6% Mo, 25–32% Cr, 53–67% Co, and small amounts of W, Al, Si, and other metals. Cr, Mo, and W enhance the alloy's strength.

Furthermore, Cr reacts with O<sub>2</sub> to form a Cr<sub>2</sub>O<sub>3</sub> layer that is 1-5 nm thick (Mohamed et al., 2023). Co-Cr alloys are commonly used for patients with missing teeth in new removable dental implants or as chrome coatings (Al-Imam et al., 2016). Co-Cr alloys are inexpensive compared to other gold or palladium alloys, additionally, these alloys have good resistance to corrosion and stretching, making them suitable for long-term use in dental applications. Moreover, these alloys can be used in orthodontics for bands, brackets, and archwires (Han et al., 2018). Co-Cr alloys typically cause low-level allergic effects and irritation, while other metal alloys have a higher risk of causing allergic reactions in oral applications (Kim et al., 2015). Cobalt-chromium (Co-Cr) alloys are coated with a layer of porcelain to enhance their strength and ability to withstand chewing pressure in dental applications (Vaicelyte et al., 2020). Ti alloys are used in implant applications, according to other Co-Cr alloys and stainless steel because Ti alloys have high strength, good corrosion resistance, and no toxicity effects (Abd-Elaziem et al., 2024). Ti6Al4V alloys were produced with the powder metallurgy method for dental applications and cylindrical shapes were characterized by the space holder method. It determined that this implant exhibited almost 40% contact trabecular bone area 200 μm diameter and 120° angle porosity (Robau-Porrúa et al., 2024). Ti-6Al-4V alloy has low density, good corrosion resistance, and excellent compatibility with bones, making it the most preferred alloy in dental applications (Chung, 2017). New titanium alloys, such as Ti-2.8Nb-15Mo and Ti-13Zr-13Nb, have been developed with a low density of 4.5 g/cm<sup>3</sup> and good corrosion resistance, making them compatible with complex tooth bone structures (Ananth et al., 2015). Neutron and gamma radiation effects were investigated for medical applications of some Ti alloys using the EpiXS, ESTAR, NGCal, and SRIM programs. Neutron interaction studies were conducted on 25.4 MeV energy thermal and 4 MeV energy fast neutrons of the investigated alloys and cortical bone. Gamma radiation interaction parameters were compared to those of cortical bone with Ti-6Al-4V-2.5Cu and Ti-6Al-4V. As a result, these alloys can be used in biomedical applications such as knee, tooth, elbow joints, and hip, for biomedical applications such as knee, hip, and elbow joints (Hiremath et al., 2023). Radioactive, micro, and mechanical properties of Ti, Ti alloys, and different elements were investigated using alloys made with Al, Sn, V, Ni, Mo, Pb, Zr, Cr, Nb, Fe, and Co through simulation studies. It was determined that Ti alloys containing Mo and Nb have good mechanical, electrical, elastic, tensile stretch, and gamma-ray attenuation properties (Taşgım, 2021).

In neutron areas, working staff who use oral implants, chrome coatings, or tooth wires can experience interactions between these materials and neutrons, resulting in secondary radiation. This radiation can have hazardous effects and may cause various health problems such as tissue destruction, oral infections, and tooth decay. Neutrons are electrically neutral, but they have a spin and magnetic moment, which allows them to affect a material's magnetic structure. Because of their neutral charge, neutrons can penetrate materials and produce secondary radiation such as gamma, alpha, and beta particles, or new radioisotope elements (Apte & Bhide, 2024). Neutron radiation has high penetrating properties in target materials, so neutron damage was investigated on some zirconium alloys. This damage may affect the microstructure and point defect development, as well as change mechanical properties and cause deformations. As a result, neutron radiation affected the interacting zirconium alloys and changed some microstructural and mechanical properties (Onimus et al., 2020).

Neutron attenuation properties such as mean free path, effective removal cross-section, half-value layer, and neutron transmission factor (NTF) were investigated for some high entropy alloys containing elements like Ta, Ti, Nb, Hf, and Zr using Monte Carlo simulation with the GEANT4 code. It was reported that the Nb<sub>25</sub>Ti<sub>25</sub>Hf<sub>25</sub>Ta<sub>25</sub> high entropy alloy has better fast neutron absorption

capacity than other alloys. According to the results, this alloy can be used in various neutron applications such as nuclear reactors, nuclear waste storage, and medical applications (Aygün & Karabulut, 2022). Newly developed superalloys were produced using metals such as rhenium (Re), nickel (Ni), iron (Fe), boron carbide (B<sub>4</sub>C), boron (B), chromium (Cr), copper (Cu), tantalum (Ta), and tungsten (W). Both gamma and neutron absorption properties were determined using the GEANT4 code, Phy-X/PSD, and WinXcom software. In addition, experimental dose measurements were made to determine the absorption ability. As a result, it was reported that these superalloys can be used in gamma and neutron applications in nuclear medicine (Aygün, 2021). In this study, epithermal and fast neutron interaction parameters, secondary radiation, and newly formed particles were determined for the most commonly used dental applications in five different implant samples. It was found which of these implants is best suited for neutron applications

## 2. Material and Methods

### 2.1. Monte Carlo simulation Geant code

The Geant4 (GEometry ANd Tracking) code can be used to simulate any particle or radiation passing through a target material to determine possible interactions. The applications included in Geant 4 can be made at any point radiation source and detector geometry designs. Additionally, new particle isotopes and secondary radiations that may occur during these interactions can be detected. Geant4 includes many different particles with energy levels ranging from low (milli-eV) to high (GeV-TeV), such as hadrons, electrons, and wave or particle radiation, and their interactions with any materials and detectors. Geant4 is used in many areas such as high energy physics, medical physics, nuclear physics, space research, accelerator devices, and the study of the effects of cosmic radiation on satellites. In addition, it is commonly used to design new samples for radiation shielding and to conduct research on new protective drugs (Agostinelli et al., 2003).

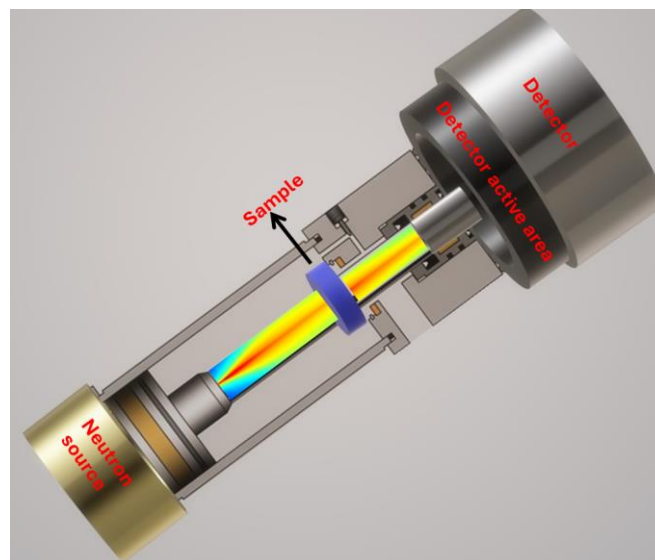


Figure 1. Geant4 simulation geometry.

### 2.2. Principles of neutron radiation protection

Neutrons have no electrical charge, so they can enter the nucleus of any target material and initiate nuclear reactions such as fission or fusion. These interactions depend on the neutron's energy levels and the type of target nucleus. Neutrons interact with the nucleus of any material, unlike X-rays, which interact with the electron shells of atoms. Therefore, neutrons are very sensitive to light element atoms such as oxygen and hydrogen, and their interaction probability is higher than that of X-rays (Podgoršak, 2009). Neutrons can make interactions such as absorption or energy transfer, elastic, inelastic scattering, neutron capture, fission, or at heavy atoms target materials which high atom

numbers. These interaction possibilities can be expressed with total macroscopic cross-sections as follows:

$$\sigma_T = \sigma_{\text{elastic scattering}} + \sigma_{\text{inelastic scattering}} + \sigma_{\text{proton}} + \sigma_{\text{alpha}} + \sigma_{\text{2neutron}} + \sigma_{\text{neutron+proton}} + \sigma_{\text{gamma}} + \sigma_{\text{fission}} \quad (1)$$

where  $\sigma$  represents the microscopic cross-section, which expresses the probability of any neutron interaction with the nuclei of target material atoms.

$$N_A = \frac{\rho}{A} N_0 \quad (2)$$

$$\sigma_A = \mu / \rho \left( \frac{A}{N_0} \right) \quad (3)$$

$$\mu = N_A \sigma_A \quad (4)$$

$$\mu = \frac{\rho}{A} N_0 \sigma_A \quad (5)$$

$N_A$  is the number of atoms of the interaction nuclide per (atom/cm<sup>3</sup>),  $N_0$  is the Avogadro's number (6.02.10<sup>23</sup>),  $\rho$  is the density of the interaction matter,  $A$  is the interaction atom molecular weight,  $\mu$  is the mass attenuation coefficient, and  $\sigma_A$  is the atomic cross-section (cm<sup>2</sup>/atom).

If neutrons interact with heavy materials such as concrete or alloys, this interaction can be expressed with a macroscopic cross-section ( $\Sigma$ ).

$$\Sigma_{Total} = \Sigma_{\text{coherent scattering}} + \Sigma_{\text{incoherent scattering}} + \Sigma_{\text{absorption cross section}} + \Sigma_{\text{captureabsorption cross section}} + \Sigma_{\text{fission absorption cross section}} + \dots \quad (6)$$

The removal cross-section  $\Sigma_R$  is like a macroscopic cross-section and can be used for neutron attenuation properties, but it doesn't give the neutron-nucleus interaction probability. This parameter can indicate fast neutron energy loss, scattering, and capture interactions, and it is lower than the macroscopic cross-section (El-Khayatt, 2010). This parameter is important for neutron protective studies, moreover, it can be used for composites, alloys, and mixture samples, and it can be calculated as follows.

$$\Sigma_R = \Sigma(\Sigma_{R/\rho})_i \quad (7)$$

$$\rho_i = w_i \rho \quad (8)$$

$w_i$  is the weight percentage and  $\rho_i$  is the density of protective material i.

When neutrons pass through any protective material, they may lose half of their numbers or energy. The material thickness at this point is expressed by the Half Value Layer (HVL), which can be calculated as follows.

$$HVL = \ln 2 / \Sigma_R \quad (9)$$

The mean free path expresses the average distance traveled by a neutron before colliding with any atoms in the target material and it can be calculated as follows.

$$\lambda = 1 / \Sigma_R \quad (10)$$

Neutrons are a type of particle radiation that can be captured, elastically or inelastically scattered by a moderator material, thereby stopping them. The stopping power of moderator materials depends on the

number of neutrons passing through the material. If this number is low, the material has a high stopping power because many collisions occur within it. Therefore, the number of incoming and passing neutrons is an important property of a moderator material. This ratio can be expressed as transmission, shown as  $I/I_0$ , where  $I_0$  is the number of incoming neutrons on the material, and  $I$  is the number of neutrons passing through the material.

### 2.3. Sample preparation

Dental alloys consist of Co-Cr metals in a high ratio. These alloys can also contain other metals such as nickel (Ni), iron (Fe), molybdenum (Mo), tungsten (W), silicon (Si), manganese (Mn), titanium (Ti), and sulfur (S). Multi-metal alloys commonly used in dentistry applications are shown in Table 1.

Table 1. Chemical composition ratios and density of the alloy used in dentistry (%)

Element	DA1 ( $\rho=8.27$ g/cm <sup>3</sup> )	DA2( $\rho=9.61$ g/cm <sup>3</sup> )	DA3( $\rho=8.03$ g/cm <sup>3</sup> )	DA4( $\rho=8.88$ g/cm <sup>3</sup> )	DA5( $\rho=7.22$ g/cm <sup>3</sup> )
Co	62.0	58.3	35.0	35.7	61.65
Cr	30.0	32.2	32.0	22.0	27.75
Mo	5.0	6.5	4.0	5.0	-
Si	1.0	1.0	0.5	0.3	1.60
Mn	1.5	-	0.5	0.7	0.5
C	0.5	0.5	0.3	0.2	-
Fe	-	-	27.7	6.0	0.5
W	-	1.5	-	5.0	8.45
Ni	-	-	-	23.0	-
Ti	-	-	-	2.0	-
S	-	-	-	0.1	-

DA: Dentistry alloys

Co and Cr metals have specific properties, and these metals are found in the human body in small quantities and are used in biochemical regulations. However, when these metals are used in implants, these metal alloys can release metal ions, which can cause toxic effects on the body (Scharf et al., 2014).

### 3. Results and Discussion

Any implant intended for use in dental and biomedical applications must have some critical properties such as nontoxicity, strong mechanical strength, corrosion resistance, and no dangerous interactions with radiation. Important parameters such as effective removal cross-section, half-value layer, mean free path and transmission number were calculated using the GEANT4 code according to the geometry in Figure 1 for the implant alloys shown in Table 1 to understand epithermal and fast neutron interactions, and the obtained results are given in Table 2-3. In addition, Table 4-8 presents the secondary radiation and new particles resulting from these neutron interactions.

The effective removal cross-section values for fast neutrons (4.5 MeV) were calculated for all alloy materials, and the results are shown in Table 2 and Figure 2. As seen in Table 2 and Figure 2, all alloy materials have effective removal cross-section values for fast neutrons, meaning that these alloys have the potential to interact with fast neutrons and can stop them. When looking at all the materials, they have effective removal cross-section values in the order of DA2 > DA4 > DA3 > DA1 > DA5. Accordingly, the material with the best neutron stopping capability is the DA2 alloy.

The half-value layer for fast neutrons was calculated using Equation 9, and the mean free path was calculated using Equation 10. The results are given in Table 2.

In neutron shielding studies, it is desired for the material to have a low half-thickness value. This is because materials that provide good shielding should be thin, which is important both volumetrically and in terms of durability (Durna et al., 2023). Especially for implants to be used inside the mouth, having the ability to stop neutrons will be advantageous for patients and individuals exposed to any neutron application. Looking at the half-thickness values given in Table 2, it is seen that the

examined alloys have the ability to stop fast neutrons. It is observed that the alloy with the lowest HVL value for fast neutrons is the DA2 material. The high ERCS value of this material also supports this result. The sample with the highest HVL value is DA5, and its ERCS value is the lowest. According to these HVL values, it was found that DA2 is the best at stopping fast neutrons. A low MFP value of a material indicates that the path neutrons can take within the material before their first collision is short, which also means that the material has good neutron stopping power (Bayram et al., 2023). Looking at the MFP values given in Table 2, it is seen that the DA2 sample has the lowest MFP value, and the DA5 sample has the highest MFP value. According to these values, it can be concluded that the DA2 sample has the best fast neutron stopping power. The ratio of neutrons that interact or pass through a material, NTR, is a guiding factor in neutron shielding studies. Again, looking at Table 2, it is seen that the DA2 sample has the lowest NTR, while the DA5 sample has the highest value. Accordingly, fewer neutrons pass through the DA2 sample, indicating that this material absorbs neutrons better. However, the high value of the DA5 sample shows that its neutron stopping potential is low. The ratio of neutrons that interact with or pass through a material, NTR, is a guiding factor in neutron shielding studies. Again, looking at Table 2, it is seen that the DA2 sample has the lowest NTR, while the DA5 sample has the highest value. Accordingly, fewer neutrons pass through the DA2 sample, indicating that this material absorbs neutrons better. However, the high value of the DA5 sample shows that its neutron stopping potential is low.

Table 2. Dentistry alloy (DA) fast neutron (4.5 MeV) attenuation parameters for 1mm thick,  $10^5$  neutron

Sample code	Fast Neutron Half value layer (cm)	Fast Neutron Mean free path $\lambda$ (mm)	Fast Neutron transmission ratio (NTR)	Fast Neutron ERCS ( $\text{cm}^{-1}$ )
DA1	$22.42 \pm 0.204$	$32.35 \pm 0.33$	0.96956	0.0309
DA2	$18.88 \pm 0.186$	$27.20 \pm 0.26$	0.96390	0.0367
DA3	$21.32 \pm 0.221$	$30.74 \pm 0.30$	0.96799	0.0325
DA4	$20.68 \pm 0.207$	$29.77 \pm 0.276$	0.96697	0.0335
DA5	$25.29 \pm 0.252$	$36.49 \pm 0.354$	0.97294	0.0274

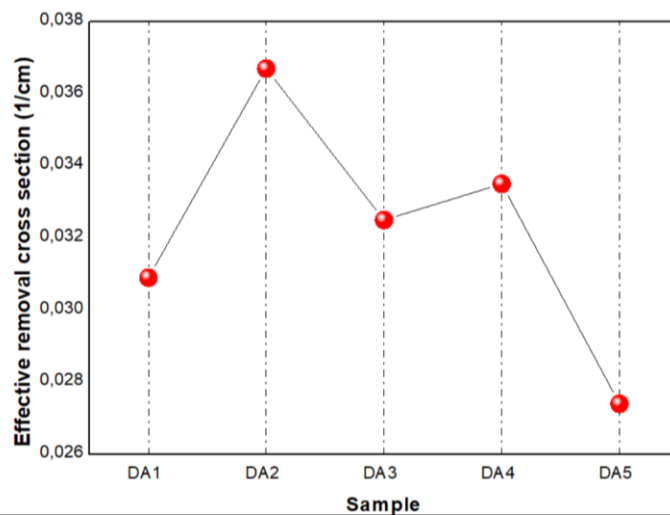


Figure 2. Theoretical 4.5 MeV fast Neutron Effective Removal Cross Sections.

A small half-value layer (HVL) value of a material is related to its ability to stop neutrons. Materials with a small HVL value absorb neutrons more effectively (Mansouri et al., 2020). According to the HVL values given in Table 3, these alloys' resistance to stopping epithermal neutrons is demonstrated. Based on these values, the DA4 sample, which has the lowest HVL value, has the best

stopping performance, while the DA5 sample, which has the highest HVL value, has the lowest stopping power.

The neutron transmission ratio (NTR) is a useful parameter, like other absorption parameters, in neutron shielding studies and predicting interactions. When examining the NTR values in Table 3, it is clear that a low ratio of the number of neutrons passing through the material to the number of neutrons sent onto the material is closely related to the material's ability to stop neutrons. According to the NTR values, the DA4 sample has the lowest NTR value, while the DA5 sample has the highest. Based on this parameter, it is determined that the material that absorbs epithermal neutrons the best is DA4, and the material that absorbs them the least is DA5.

Table 3. Dentistry alloy (DA) epithermal neutron (0.25 eV) attenuation parameters for 1mm thick,  $10^5$  neutron

Sample code	Epithermal Neutron Half value layer (cm)	Epithermal Neutron Mean free path $\lambda$ (mm)	Epithermal Neutron Transmission Ratio NTR ( $I/I_0$ )	Epithermal Neutron ERCS ( $\text{cm}^{-1}$ )
DA1	$7.21 \pm 0.78$	$10.41 \pm 0.13$	0.90846	0.0960
DA2	$6.45 \pm 0.64$	$9.31 \pm 0.93$	0.89821	0.1073
DA3	$7.86 \pm 0.76$	$11.35 \pm 0.59$	0.91563	0.0881
DA4	$6.12 \pm 0.61$	$8.84 \pm 0.89$	0.89303	0.1131
DA5	$8.27 \pm 0.82$	$11.94 \pm 0.11$	0.91970	0.0837

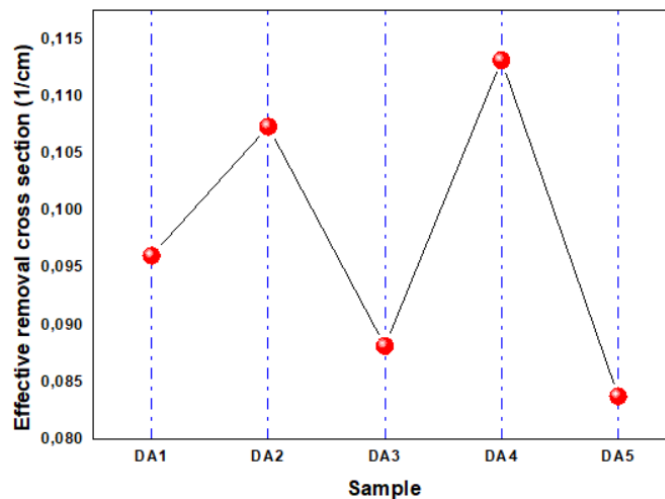


Figure 3. Theoretical 0.25 eV epithermal neutron effective removal cross sections.

Based on the results presented in Table 3 and Figure 3, it has been determined that all DA alloys possess ERCS values. Accordingly, it is observed that these alloys have the potential to interact with epithermal neutrons, meaning they have the capability to stop epithermal neutrons. The material with a higher ERCS value has a greater power to stop neutrons (Kursun et al., 2023). Accordingly, there is a relationship among the ERCS values of all materials, specifically between  $DA4 > DA2 > DA1 > DA3 > DA5$ . Based on this, the DA4 alloy has the highest stopping power against epithermal neutrons, while the DA5 alloy has the lowest stopping power.

The mean free path facilitates material selection in neutron shielding studies. A small value of this parameter for a material indicates its capacity to stop neutrons. When examining the values given in Table 3, it is evident that the short distances traveled by epithermal neutrons through the alloys without interaction demonstrate these materials' ability to stop epithermal neutrons. The fact that the DA4 sample has the lowest MFP value in the table clearly proves that this alloy has the highest capacity to stop epithermal neutrons. Conversely, the DA5 sample, which has the highest MFP value in the table, has the lowest capacity to stop epithermal neutrons compared to the other alloys.

Tables 4 provide the secondary radiations and radioactive particles resulting from the interaction of the DA1 alloy with both fast and epithermal neutrons. According to these results, it is

understood that the particles produced when this alloy sample interacts with both fast and epithermal neutrons will not have very high energies.

Table 4. Secondary particles and radiations emerge from the DA1 sample by fast and epithermal neutrons

Emerge isotopes and secondary radiations	fast neutrons		epithermal neutrons	
	Quantity (core/cm <sup>3</sup> )	Energy (keV)	Quantity (core/cm <sup>3</sup> )	Energy (keV)
C12	24	379.36	-	-
C13	1	274.78	-	-
Co59	1807	71.77	3009	0.0500
Co60	2	72.76	4740	257.64
Cr50	50	72.66	24	0.0506
Cr51	-	-	57	831.24
Cr52	857	80.04	677	0.0517
Cr53	91	58.23	251	203.91
Cr54	27	89.37	127	801.13
Fe59	3	103.2	-	-
Mn55	52	88.15	27	0.0598
Mn56	-	-	50	558.01
Mo101	-	-	2	156.55
Mo100	15	28.84	12	0.0716
Mo92	19	44.96	20	0.0406
Mo94	10	43.03	13	0.0255
Mo95	17	60.28	24	0.0331
Mo96	10	26.31	39	81.132
Mo97	7	65.164	15	0.0625
Mo98	23	49.70	37	0.0444
Si28	31	135.25	29	0.0755
Si29	1	10.88	1	0.0502
Si30	2	302.4	-	-
V50	5	163.3	-	-
e-	-	-	2	10.623
gamma	3512	1.019	12810	3.0202
neutron	1224	1.499	-	-
proton	8	3.572	-	-

Tables 5 present the secondary radiations and radioactive particles that can result from the interactions of the DA2 alloy with both fast and epithermal neutrons. According to the calculations, the DA2 sample has the best absorption capability against fast neutrons among all alloy materials. It has been determined that no high-energy radiation or radioactive particles will form as a result of the interaction of this material with fast and epithermal neutrons.



Table 5. Secondary particles and radiations emerge from the DA2 sample by fast and epithermal neutrons

Emerge isotopes and secondary radiations	fast neutrons		epithermal neutrons	
	Quantity (core/cm <sup>3</sup> )	Energy (keV)	Quantity (core/cm <sup>3</sup> )	Energy (keV)
C12	33	373.17	105	0.1008
C13	1	544.72	3	0.0750
Co59	2020	73.284	3280	0.0505
Co60	1	81.86	5061	255.23
Cr50	55	55.755	35	0.0590
Cr51	-	-	69	798.63
Cr52	1121	74.167	883	0.0518
Cr53	111	71.393	288	229.93
Cr54	27	86.271	159	943.33
Cr55	-	-	1	385.36
Fe59	2	122	-	-
Mo100	25	39.177	17	0.0430
Mo101	-	-	1	150.71
Mo92	21	46.055	31	0.0425
Mo94	21	72.274	25	0.0437
Mo95	15	51.542	38	0.3511
Mo96	24	53.562	43	55.183
Mo97	15	30.694	20	0.1253
Mo98	37	48.616	50	0.0584
Si28	41	187.49	31	0.0603
Si29	1	10.887	1	0.1251
Si30	2	329.93	1	0.0755
V50	8	166.03	-	-
W182	10	17.874	10	0.0293
W183	2	329.93	7	70.591
W184	7	23.015	7	0.0482
W185	-	-	1	314.89
W186	10	26.892	-	-
W187	-	-	12	37.865
e-	-	-	1	12.991
gamma	4061	1.0194	13643	3.0477
neutron	1432	1.5291	-	-
proton	10	3.5823	-	-

Tables 6 present the secondary radiations and radioactive particles that may result from the interactions of the DA3 alloy sample with both fast and epithermal neutrons. According to these tables, the radiation emitted after the interaction of this material with fast and epithermal neutrons does not pose a significant threat to human health. However, prolonged exposure to this level of radiation may still pose health risks.

Table 6. Secondary particles and radiations emerge from the DA3 sample by fast and epithermal neutrons

Emerge isotopes and secondary radiations	fast neutrons		epithermal neutrons	
	Quantity (core/cm <sup>3</sup> )	Energy (keV)	Quantity (core/cm <sup>3</sup> )	Energy (keV)
C12	7	491.36	58	0.0876
C13	2	129.89	-	-
Co59	1028	70.415	1718	0.0513
Co60	1	76.972	2624	260.48
Cr50	52	63.749	32	0.0629
Cr51	-	-	55	842.19
Cr52	927	82.074	736	0.0520
Cr53	121	75.384	266	201.97
Cr54	28	74.088	139	902.08
Fe54	48	64.384	28	0.0463
Fe55	-	-	4	950.7
Fe56	823	67.85	2478	0.0507
Fe57	21	77.844	146	614.35
Fe58	6	75.941	5	271.8
Fe59	5	138.35	-	-
Mn54	8	189.86	-	-
Mn55	14	62.91	9	0.0334
Mn56	-	-	16	811.66
Mo100	8	41.187	11	0.0337
Mo92	14	41.187	18	0.0433
Mo94	6	22.696	5	0.0397
Mo95	6	26.468	16	0.0570
Mo96	12	55.785	26	75.176
Mo97	11	50.471	15	0.0826
Mo98	25	47.667	17	0.7033
Si28	20	171.59	14	0.0683
Si29	1	76.4	-	-
Si30	1	62.334	1	0.1699
V50	6	241.98	-	-
gamma	3027	1.0985	7598	3.2063
neutron	1173	1.5816	-	-
proton	19	4.0003	-	-

In Table 7, the secondary radiations and particles that will occur for both fast and epithermal neutrons are given for the DA4 alloy, which has the best epithermal neutron stopping capability compared to other alloys. According to these results, the energies of the particles and radiations that will occur are not very high. Especially in epithermal neutron interactions, gamma rays are the only secondary radiation produced, and their energies are very low. According to these results, the DA4 alloy can be easily used in epithermal neutron applications.

Table 7. Secondary particles and radiations emerge from the DA4 sample by fast and epithermal neutrons

Emerge isotopes and secondary radiations	fast neutrons		epithermal neutrons	
	Quantity (core/cm <sup>3</sup> )	Energy (keV)	Quantity (core/cm <sup>3</sup> )	Energy (keV)
C12	11	314.26	36	0.0884
C13	-	-	1	0.0431
Co58	54	150.63	-	-
Co59	1175	69.387	1835	0.0498
Co60	-	-	2947	273.29
Cr50	46	57.537	20	0.0464
Cr51	-	-	47	827.5
Cr52	667	82.078	547	0.0537
Cr53	77	68.961	195	156.13
Cr54	21	50.772	105	876.11
Fe54	9	115.48	8	0.0652
Fe55	3	252.57	1	958.61
Fe56	221	70.988	610	0.0528
Fe57	7	40.92	42	568.07
Fe58	-	-	1	527.96
Fe59	2	79.886	-	-
Mn55	29	72.463	11	0.0665
Mn56	9	56.162	20	538.68
Mo100	-	-	9	0.0225
Mo92	13	53.151	28	0.0509
Mo94	5	59.79	15	0.0364
Mo95	22	36.441	29	2.3321
Mo96	18	45.886	25	75.683
Mo97	12	40.697	16	0.0353
Mo98	19	43.497	40	1.9996
Ni58	477	68.079	3482	0.0497
Ni59	-	-	153	865.86
Ni60	186	67.73	64	0.0498
Ni61	11	61.623	56	325.37
Ni62	12	45.92	79	0.0423
Ni63	-	-	23	446.16
Ni64	3	88.897	1	0.0295
S32	4	118.56	1	0.1014
Si28	6	120.51	5	0.0504
Si30	-	-	1	0.0130
Ti46	-	-	2	0.0369
Ti47	-	-	3	0.0341
Ti48	53	81.701	53	22.022
Ti49	-	-	28	385.65
Ti50	-	-	6	0.0637
V50	4	127.36	-	-
W182	-	-	45	0.0426
W183	-	-	33	62.41
W184	-	-	24	21.11
W185	-	-	1	98.09
W186	30	21.463	-	-
W187	-	-	49	64.66

Table 7. Secondary particles and radiations emerge from the DA4 sample by fast and epithermal neutrons (continued)

Emerge isotopes and secondary radiations	fast neutrons		epithermal neutrons	
	Quantity (core/cm <sup>3</sup> )	Energy (keV)	Quantity (core/cm <sup>3</sup> )	Energy (keV)
alpha	6	5.925	-	-
gamma	3495	1.0275	8455	3.312
neutron	1262	1.5949	-	-
proton	60	4.1402	-	-

In Table 8, the secondary radiations and radioactive particles that will occur as a result of the interaction of the DA5 alloy sample with fast and epithermal neutrons are given. According to this, gamma rays, neutrons, and protons are formed due to the interaction of the DA5 alloy with fast neutrons, but their energies are also low. It has been determined that only gamma rays with low energy levels are formed due to the interaction of the DA5 alloy with epithermal neutrons, and new radioactive particles with low energies are also formed.

Table 8. Secondary particles and radiations emerge from the DA5 sample by fast and epithermal neutrons

Emerge isotopes and secondary radiations	fast neutrons		epithermal neutrons	
	Quantity (core/cm <sup>3</sup> )	Energy (keV)	Quantity (core/cm <sup>3</sup> )	Energy (keV)
Co59	1631	72.506	2667	0.0504
Co60	-	-	4122	256.5
Cr50	34	89.198	20	0.0474
Cr51	-	-	36	796.95
Cr52	729	74.746	560	0.0523
Cr53	81	73.332	232	165.2
Cr54	13	91.719	111	871.78
Fe56	8	69.234	40	0.0544
Fe57	1	135.45	1	654.47
Fe59	3	171.92	-	-
Mn55	11	47.772	9	0.0395
Mn56	-	-	40	420.22
Si28	68	172.87	52	0.0605
Si29	2	102.72	2	0.0438
Si30	1	99.703	-	-
V50	3	280	-	-
W180	-	-	1	0.0378
W182	37	17.813	44	0.0343
W183	17	14.407	41	67.554
W184	38	19.405	24	10.897
W185	-	-	3	124.9
W186	29	14.781	-	-
W187	-	-	51	60.847
gamma	3183	997.18	11227	2.9973
neutron	1107	1.5368	-	-
proton	6	3.5969	-	-

All results indicated that all DA alloys have absorption capacities against fast and epithermal neutrons. Among all DA alloys, the DA2 alloy sample has the best absorption performance for fast neutrons. When examining the chemical composition of this alloy given in Table 1, it is seen that it has both the highest density and a higher content of Co and Cr compared to the other alloys. This is because Co and Cr elements have an effective absorption coefficient against fast neutrons (Sriwongsa et al., 2020). Similarly, the DA4 alloy sample has the best absorption capacity against epithermal neutrons. The probable reason for this, when looking at Table 1, is that it has the highest density after the DA2 sample and, unlike the other samples, contains Ni and Ti elements because Ni and Ti elements have an effective absorption capability for epithermal neutrons (Aygün & Karabulut, 2022).

#### 4. Conclusion

In this study, particularly in the field of dentistry, the interactions of implant alloys, used to replace decayed and completely lost teeth, with fast and epithermal neutrons and the secondary radiations and particles formed during these interactions were examined. Important attenuation parameters such as HVL, NTR, ERCS, and MFP, which are neutron interaction parameters, were theoretically calculated using the Geant4 code. It was determined that all dental alloy samples have absorption ability against both epithermal and neutron radiation. These alloys are used in both dentistry and many medical applications. If a person uses these alloy implants or prostheses, and is in an area where neutron radiation applications are located, these interactions may occur, leading to new radiation and radioactive particles, which can have hazardous effects on health. So, the interactions of these alloys with neutrons and the new radiation produced with radioactive particles must be understood. According to these results, it was found that the DA2 alloy sample has better absorption capacity against fast neutron radiation, while the DA4 alloy sample has better absorption capacity against epithermal neutron radiation compared to the other alloys. In addition to these absorption parameters, it was determined that none of the alloy samples produced or contained any high-energy secondary radiation or radioactive particles that could be harmful to people's health. Radiation absorption dose limits vary depending on the type and energy of the radiation. Every organ has specific radiation dose limits for acute radiation effects, for instance, 1 Sv (1000 mSv). This is a high dose level, but in this study, the second radiation dose value was lower than this level. It is suggested that the DA2 alloy sample can be used for implants and other medical therapies in any neutron applications.

#### References

- Abd-Elaziem, W., Darwish, M. A., Hamada, A., & Daoush, W. M. (2024). Titanium-based alloys and composites for orthopedic implants applications: A comprehensive review. *Materials & Design*, 241, 112850. <https://doi.org/10.1016/j.matdes.2024.112850>
- Agostinelli, S., Allison, J., Amako, K., Apostolakis, J., Araujo, H., Arce, P., ... & Zschesche, D. (2003). GEANT4 - A simulation toolkit. *Nuclear Instruments and Methods in Physics Research Section A: Accelerators, Spectrometers, Detectors and Associated Equipment*, 506(3), 250-303. [https://doi.org/10.1016/S0168-9002\(03\)01368-8](https://doi.org/10.1016/S0168-9002(03)01368-8)
- Al-Imam, H., Benetti, A. R., Özhayat, E. B., Pedersen, A. M. L., Johansen, J. D., Thyssen, J. P., ... & Gotfredsen, K. (2016). Cobalt release and complications resulting from the use of dental prostheses. *Contact Dermatitis*, 75(6), 377-383. <https://doi.org/10.1111/cod.12649>
- Ananth, H., Kundapur, V., Mohammed, H. S., Anand, M., Amarnath, G. S., & Mankar, S. (2015). A review on biomaterials in dental implantology. *International Journal of Biomedical Science: IJBS*, 11(3), 113-120.
- Apte, K., & Bhide, S. (2024). Advanced radiation shielding materials: In S. Verma, & A. K. Srivastava (Eds.), *Basics of radiation* (pp. 1-23). Elsevier. <https://doi.org/10.1016/B978-0-323-95387-0.00013-3>
- Aygün, B. (2021). Neutron and gamma radiation shielding Ni based new type super alloys development and production by Monte Carlo Simulation technique. *Radiation Physics and Chemistry*, 188, 109630. <https://doi.org/10.1016/j.radphyschem.2021.109630>

- Aygün, B., & Karabulut, A. (2022). Investigation of epithermal and fast neutron shielding properties of some high entropy alloys containing Ti, Hf, Nb, and Zr. *Eastern Anatolian Journal of Science*, 8(2), 37-44.
- Bayram, S., Aygün, B., Karadayi, M., Alaylar, B., Güllüce, M., & Karabulut, A. (2023). Determination of toxicity and radioprotective properties of bacterial and fungal eumelanin pigments. *International Journal of Radiation Biology*, 99(11), 1785-1793. <https://doi.org/10.1080/09553002.2023.2204957>
- Chung, D. D. L. (2017). Carbon-matrix composites. In *Carbon composites, composites with carbon fibers, nanofibers and nanotubes* (pp. 387-466). Elsevier. <https://doi.org/10.1016/B978-0-12-804459-9.00007-5>
- Durna, D., Aygün, B., Genişel, M., & Singh, V. P. (2023). Investigation of the neutron radiation protective properties of chlorophyll and carotenoid. *Radiation Physics and Chemistry*, 208, 110873. <https://doi.org/10.1016/j.radphyschem.2023.110873>
- El-Khayatt, A. M. (2010). Calculation of fast neutron removal cross-sections for some compounds and materials. *Annals of Nuclear Energy*, 37(2), 218-222. <https://doi.org/10.1016/j.anucene.2009.10.022>
- Han, X., Sawada, T., Schille, C., Schweizer, E., Scheideler, L., Geis-Gerstorfer, J., ... & Spintzyk, S. (2018). Comparative analysis of mechanical properties and metal-ceramic bond strength of Co-Cr dental alloy fabricated by different manufacturing processes. *Materials*, 11(10), 1801. <https://doi.org/10.3390/ma11101801>
- Hiremath, G. B., Singh, V. P., Patil, P. N., Ayachit, N. H., & Badiger, N. M. (2023). Investigation of the nuclear radiation parameters of some Ti alloys for biomedical applications. *Radiation Effects and Defects in Solids*, 179 (3-4), 301-314. <https://doi.org/10.1080/10420150.2023.2265020>
- Kassapidou, M., Stenport, V. F., Hjalmarsson, L., & Johansson, C. B. (2017). Cobalt-chromium alloys in fixed prosthodontics in Sweden. *Acta Biomaterialia Odontologica Scandinavica*, 3(1), 53-62. <https://doi.org/10.1080/23337931.2017.1360776>
- Kim, T. W., Kim, W. I., Mun, J. H., Song, M., Kim, H. S., Kim, B. S., Kim, M. B., & Ko, H. C. (2015). Patch testing with dental screening series in oral disease. *Annals of Dermatology*, 27(4), 389-393. <https://doi.org/10.5021/ad.2015.27.4.389>
- Kursun, C., Gao, M., Guclu, S., Gaylan, Y., Parrey, K. A., & Yalcin, A. O. (2023). Measurement on the neutron and gamma radiation shielding performance of boron-doped titanium alloy Ti<sub>50</sub>Cu<sub>30</sub>Zr<sub>15</sub>B<sub>5</sub> via arc melting technique. *Heliyon*, 9(11), 1-11. <https://doi.org/10.1016/j.heliyon.2023.e21696>
- Mansouri, E., Mesbahi, A., Malekzadeh, R., Ghasemi Janghjo, A., & Okutan, M. (2020). A review on neutron shielding performance of nano - composite materials. *International Journal of Radiation Research*, 18(4), 611-622. <http://dx.doi.org/10.52547/ijrr.18.4.611>
- Mohamed, L. Z., Elsayed, A. H., Elkady, O. A., & Abolkassem, S. A. (2023). Physico-mechanical, microstructure, and chemical properties of Si/Ti/Nb additions to CoCrMoW medium entropy alloys. *Journal of Materials Research and Technology*, 24, 9897-9914. <https://doi.org/10.1016/j.jmrt.2023.05.198>
- Nazarov, K. M., Muhametuly, B., Kenzhin E. A., Kichanov, S. E., Kozlenko, D. P., Lukin, E. V., & Shaimerdenov, A. (2020). New neutron radiography and tomography facility TITAN at the WWR-K reactor. *Nuclear Instruments and Methods in Physics Research Section A (NIM-A)*, 982, 164572. <https://doi.org/10.1016/j.nima.2020.164572>
- Onimus, F., Doriot, S., & Béchade, J. L. (2020). Radiation effects in zirconium alloys. In R. J. M. Konings, & R. E. Stoller (Eds.), *Comprehensive nuclear materials* (pp. 1-56). Elsevier. <https://doi.org/10.1016/B978-0-12-803581-8.11759-X>
- Podgoršak, E. B. (2009). Interactions of neutrons with matter. In *Radiation physics for medical physicists. Biological and Medical Physics, Biomedical Engineering* (pp. 429-49). Springer. [https://doi.org/10.1007/978-3-642-00875-7\\_9](https://doi.org/10.1007/978-3-642-00875-7_9)
- Robau-Porrúa, A., González, J. E., Rodríguez-Guerra, J., González-Mederos, P., Navarro, P., De La Rosa, J. E., ... & Torres, Y. (2024). Biomechanical behavior of a new design of dental implant: Influence of the porosity and location in the maxilla. *Journal of Materials Research and Technology*, 29, 3255-3267. <https://doi.org/10.1016/j.jmrt.2024.02.091>

- Scharf, B., Clement, C., Zolla, V., Perino, G., Yan, B., Gokhan Elci, S., ... & Santambrogio, L. (2014). Molecular analysis of chromium and cobalt-related toxicity. *Scientific Reports*, 4, 5729. <https://doi.org/10.1038/srep05729>
- Sriwongsa, K., Glumglomchit, P., Wananuraksakul, T., Pimprakhon, A., Hanchana, T., & Ravangvong, S. (2020). Simulation of shielding parameters of some high entropy alloys containing energies for gamma ray and fast neutron. *Research Journal Rajamangala University of Technology Thanyaburi*, 19, 97-105.
- Taşgın, Y. (2021). Investigation of microstructural and mechanical properties of different titanium alloys for gamma radiation properties and implant applications. *Journal of Material Engineering and Performance*, 30, 6203-6223. <https://doi.org/10.1007/s11665-021-05830-0>
- Vaicelyte, A., Janssen, C., Le Borgne, M., Grosgeat, B. (2020). Cobalt–chromium dental alloys: Metal exposures, toxicological risks, CMR classification, and EU regulatory framework. *Crystals*, 10(12), 1151. <https://doi.org/10.3390/cryst10121151>